Eur. Phys. J. Plus (2023) 138:1012
https://doi.org/10.1140/epjp/s13360-023-04644-4

THE EUROPEAN PHYSICAL JOURNAL PLUS

Regular Article

Spatial potential of arbitrary uniformly charged polygons

Chen Sheng[1,a], **Lu Junyi**[1], **Chang Xin**[2], **Wu Yanyi**[1], **Teng Baohua**[1,2]

[1] School of Physics, University of Electronic Science and Technology of China, Chengdu 611731, People's Republic of China
[2] Yingcai Experimental School, University of Electronic Science and Technology of China, Chengdu 611731, People's Republic of China

Received: 29 August 2023 / Accepted: 31 October 2023

Abstract In this paper, a unified analytical method for calculating the potential of any uniformly charged polygon is proposed. The principle of dividing an arbitrary N-sided polygon into N triangles is firstly determined by using the superposition theorem. Then the plane electric potential of the uniformly charged N-sided polygon is equivalent to the electric potentials at the vertices of N triangles, and further the space electric potential of the uniformly charged N-sided polygon is equivalent to the electric potentials on the perpendicular lines at the vertices of N triangles. As an application of this method, the analytical expressions for the center and vertex potentials of a uniformly charged regular N-sided polygon are obtained, and the equipotential lines of the plane and space potentials of an arbitrary N-sided polygon are plotted. The results show that the equipotential lines can always reflect the shape characteristics of charged bodies.

1 Introduction

Basic education is not only to provide students with extensive scientific knowledge, but also to cultivate students' ability to analyze and solve problems. Adopting a reverse design and thinking from the learner's perspective is the most efficient way to do this. Therefore, teaching models such as the "peer learning" emerged in modern teaching, which is more innovative and better than traditional teaching [1, 2]. By creating a topic that is based on the textbook but with a focus on practicality and generality, and by conducting small-class and small-group discussions in the classroom, teachers can stimulate students' curiosity, enable them to learn from each other, and strengthen their understanding of physical processes and the laws, making it possible to solve more complex physics problems more efficiently, and the teaching more widely applicable to a wide range of students.

The solution of electrostatic potential is an important problem in electromagnetics teaching. Theoretically, the electric field intensity and electric field force of an electric charge at the point can be obtained by knowing the electric potential at any point, and then the relationship between electric field and electric charge distribution can be explored. For highly regular three-dimensional charged bodies such as spheres and infinitely long cylinders, Gauss's law is generally used to solve for the electric field distribution and further obtain the potential distribution. However, when the charged body degenerates to a two-dimensional finite plane, the electric field cannot be seen as uniformly constant in the direction perpendicular to the plane, and thus the electric field distribution cannot be accurately solved by Gauss's law. Therefore, only the potential distribution of highly symmetric figures or special points is often discussed in the current college physics exercises, such as rectangles and disks [3, 4]. In addition, students are often confused by several choices when solving for the potential of a uniformly charged body: (1) the differential element; (2) the coordinate system; (3) the point of integration of the field.

In contrast to the direct integral method ($V = \int dq/4\pi\varepsilon_0|\boldsymbol{r} - \boldsymbol{r}|$), which uses point charge microelements, it is important to select the appropriate microelements for different shaped charged bodies [5–8], e.g., a long thin strip of microelements for a square plane, or circular microelements for a disk potential. This not only avoids complex integral calculations, but also makes it easier to obtain analytical solutions. The application of right-angle coordinate systems to the solution of spatial potentials usually involves elliptic integrals, whereas polar coordinate systems can avoid integral singularities to solve for the potential at the vertices of uniformly charged triangles. The barycentric coordinate systems can solve for the analytical expressions of spatial potentials for non-symmetric triangles [7, 9], but it requires great mathematical skill. There is still no unified solution to the problem of obtaining analytical expressions for the spatial potential of arbitrary polygons in the usual coordinate system by means of less complex integration calculations, the solution to the potential for complex polygons still relies on numerical integration. However, problems are often encountered in performing numerical calculations. On the one hand, in order to obtain a high-precision numerical solution, it is required that the integral region should approach the original figure infinitely, that is, the step size should be small enough and the grid should be dense enough [10]; On the other hand, in order to avoid singularity, it is necessary to avoid the coincidence

[a] e-mail: chensheng9807@163.com (corresponding author)

Published online: 13 November 2023

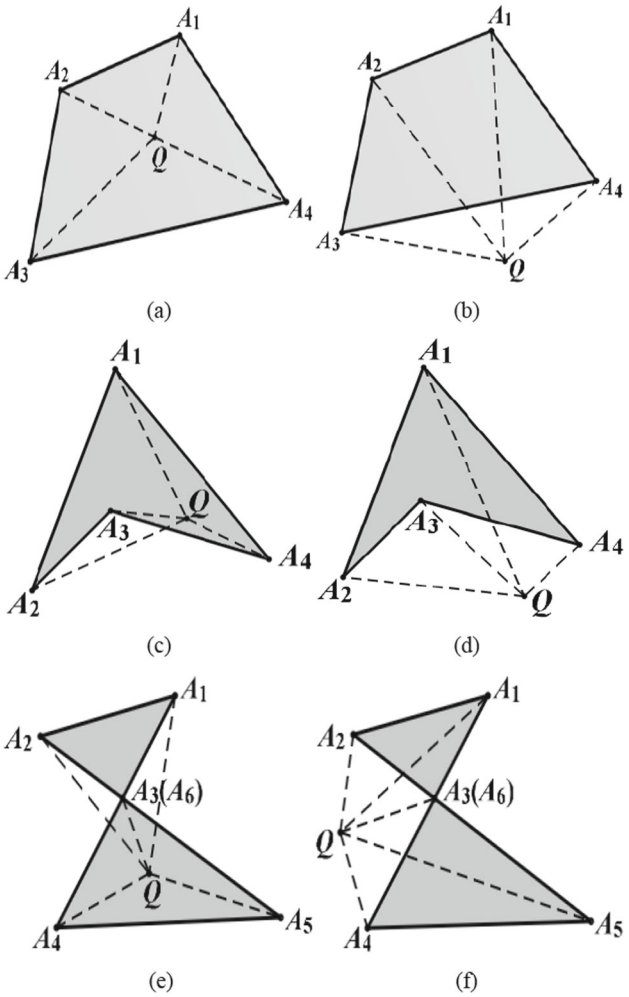

Fig. 1 Relationship between the divided triangles of polygon and the field point

between the field point and the source point [9], which makes the numerical calculation slightly rough. At the same time, the amount of numerical calculation is also very large, which requires a lot of time and computing resources.

Therefore, it is necessary to explore the analytical expression for the spatial potential of an arbitrary uniformly charged polygon [11]. Based on the superposition theorem of potential, a rule for dividing an arbitrary N-sided shape into N triangles is proposed firstly in this article. Then the plane potential of the uniformly charged polygon is obtained by analyzing the potentials of triangle vertices, the space potential of the uniformly charged polygon is obtained from the potential on the vertical line of the vertex of the triangle. Finally, the potentials of the center and vertex of the uniformly charged regular N-sided polygon are calculated, and the equipotential lines of the plane potential and the space potential of the N-sided polygon are drawn.

2 Rules for triangle segmentation of arbitrary polygon

Unlike triangles, which have a fixed shape, polygons are extremely complex, with convex polygons (Fig. 1a and b), concave polygons (Fig. 1c and d), self-intersecting polygons (Fig. 1e and f) and many other cases. Previous literature has only discussed the solution of the potential for convex polygons, which are divided into different ways for in-plane and out-plane, or only studied the analytical solution of the potential for highly symmetric shapes such as rectangles. In order to solve for the potential of an arbitrary polygonal plane, it is necessary to determine a unified principle of dividing the plane into several triangles, so that the potential of any uniformly charged polygon can be obtained by using the superposition theorem. Because quadrilateral is the simplest figure that can contain the characteristics of the polygon, without losing generality we take irregular quadrilateral (Fig. 1a–f) (self-intersecting quadrilateral must be regarded as a hexagon) as an example to determine the division rules and the solution steps for the potential at any field point $\boldsymbol{Q}$ in its plane:

(i) Specify that the vertices are numbered counterclockwise and designated as A_i ($i = 1, 2\ldots N$);

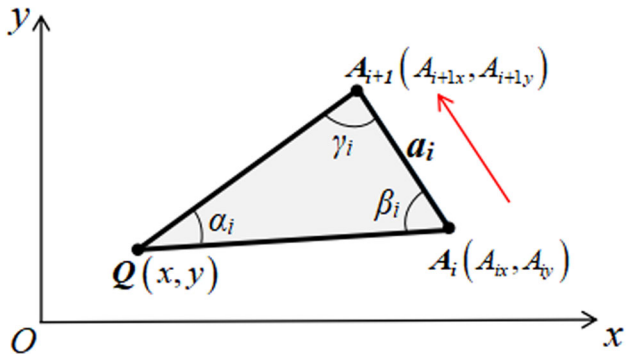

Fig. 2 Triangle ΔQA_iA_{i+1} in the XOY plane

(ii) Connect the field point $\boldsymbol{Q}$ with each adjacent vertex A_i and A_{i+1} in turn and divide polygon into N triangles ΔQA_iA_{i+1} (if the point $\boldsymbol{Q}$ is located on the edge, it is equivalent to zero triangle at this time);
(iii) When traveling counterclockwise, the triangle ΔQA_iA_{i+1} in (ii) is positively charged if the $\boldsymbol{Q}$ point lies to the left of the directed segment $\overrightarrow{A_iA_{i+1}}$, and the triangle ΔQA_iA_{i+1} in (ii) is negatively charged or seen as subtracting the positively charged ΔQA_iA_{i+1} if the $\boldsymbol{Q}$ point lies to the right of the directed segment $\overrightarrow{A_iA_{i+1}}$;
(iv) Accumulate the potentials of N uniformly charged triangles ΔQA_iA_{i+1} at vertices $\boldsymbol{Q}$.

For the above six cases (Figs. 1(a–f), the$\boldsymbol{Q}$-point potential can be recorded as:

(a) $V_Q = V_{QA_1A_2} + V_{QA_2A_3} + V_{QA_3A_4} + V_{QA_4A_1}$
(b) $V_Q = V_{QA_1A_2} + V_{QA_2A_3} - V_{QA_3A_4} + V_{QA_4A_1}$
(c) $V_Q = V_{QA_1A_2} - V_{QA_2A_3} + V_{QA_3A_4} + V_{QA_4A_1}$
(d) $V_Q = V_{QA_1A_2} - V_{QA_2A_3} - V_{QA_3A_4} + V_{QA_4A_1}$
(e) $V_Q = V_{QA_1A_2} - V_{QA_2A_3} + V_{QA_3A_4} + V_{QA_4A_5} + V_{QA_5A_6} - V_{QA_6A_1}$
(f) $V_Q = V_{QA_1A_2} - V_{QA_2A_3} - V_{QA_3A_4} + V_{QA_4A_5} + V_{QA_5A_6} + V_{QA_6A_1}$

Based on the periodicity of the polygon vertices, i.e., $\boldsymbol{A_{N+1} = A_1}$, the plane potential of a uniformly charged polygon can be written in principle as:

$$V_Q = \sum_{i=1}^{N} \delta_i V_{QA_iA_{i+1}} \tag{1}$$

where $\delta_i = \pm 1$, determined by the shape of polygon and the position of field points.

3 Plane potential of a uniformly charged polygon

Assume that the polygon $\boldsymbol{A_1A_2 \ldots A_N}$ lies in the XOY plane, where the length of the side opposite the vertex $\boldsymbol{Q}$ of any triangle ΔQA_iA_{i+1} is $\boldsymbol{a_i}$ ($\equiv \overline{A_iA_{i+1}}$), and the included angles are denoted asα_i, β_i and γ_i in counterclockwise order, respectively, as shown in Fig. 2.

According to the analytical expression for the potential at the vertices of the uniformly charged triangle [4, 12], the potential of the field point $\boldsymbol{Q}(x, y)$ in the plane where the polygon $\boldsymbol{A_1A_2 \ldots A_N}$ is located can be written as:

$$V(x, y) = \frac{\sigma}{4\pi\varepsilon_0} \sum_{i=1}^{N} \frac{\delta_i a_i \sin\beta_i \sin\gamma_i}{\sin\alpha_i} \ln\left(\cot\left(\frac{\beta_i}{2}\right)\cot\left(\frac{\gamma_i}{2}\right)\right) \tag{2}$$

The derivation of Eq. (2) is presented in Appendix A. Here σ is the charge surface density, ε_0 is the vacuum dielectric constant, and

$$\begin{aligned}
\alpha_i &= \arccos\left(\frac{\overline{QA_i}^2 + \overline{QA_{i+1}}^2 - \overline{A_iA_{i+1}}^2}{2\overline{QA_i}\cdot\overline{QA_{i+1}}}\right) \\
\beta_i &= \arccos\left(\frac{\overline{QA_i}^2 + \overline{A_iA_{i+1}}^2 - \overline{QA_{i+1}}^2}{2\overline{QA_i}\cdot\overline{A_iA_{i+1}}}\right) \\
\gamma_i &= \arccos\left(\frac{\overline{A_iA_{i+1}}^2 + \overline{QA_{i+1}}^2 - \overline{QA_i}^2}{2\overline{A_iA_{i+1}}\cdot\overline{QA_{i+1}}}\right)
\end{aligned} \tag{3}$$

Considering that the potential generated at point $\boldsymbol{Q}$ by ΔQA_iA_{i+1} is zero when the field point $\boldsymbol{Q}$ lies on $\overline{A_iA_{i+1}}$ edge, δ_i can also be expressed as:

$$\delta_i = \mathrm{sgn}\left[(A_{i+1x} - A_{ix})(y - A_{iy}) - (A_{i+1y} - A_{iy})(x - A_{ix})\right] \tag{4}$$

For any uniformly charged quadrilateral $\boldsymbol{A_1A_2A_3A_4}$ (Fig. 1(a)-(d)), if its vertices coordinates are $\boldsymbol{A_1}$ (x_1, y_1), $\boldsymbol{A_2}$ (x_2, y_2), $\boldsymbol{A_3}$ (x_3, y_3) and $\boldsymbol{A_4}$ (x_4, y_4) in turn, the potential at any point (x, y) in its plane can be analytically expressed as:

$$V(x,y) = \frac{\sigma}{4\pi\varepsilon_0}\sum_{i=1}^{4}\delta_i H_i \ln\left(\cot\left(\frac{\beta_i}{2}\right)\cot\left(\frac{\gamma_i}{2}\right)\right) \tag{5}$$

where

$$H_i = \sqrt{(x_{i+1} - x_i)^2 + (y_{i+1} - y_i)^2}\sin\beta_i \sin\gamma_i / \sin\alpha_i$$

$$\delta_i = \mathrm{sgn}[(x_{i+1} - x_i)(y - y_i) - (y_{i+1} - y_i)(x - x_i)]$$

$$\alpha_i = \arccos\left(\frac{(x - x_i)^2 + (y - y_i)^2 + (x - x_{i+1})^2 + (y - y_{i+1})^2 - (x_{i+1} - x_i)^2 - (y_{i+1} - y_i)^2}{2\sqrt{(x - x_i)^2 + (y - y_i)^2}\sqrt{(x - x_{i+1})^2 + (y - y_{i+1})^2}}\right)$$

$$\beta_i = \arccos\left(\frac{(x - x_i)^2 + (y - y_i)^2 + (x_{i+1} - x_i)^2 + (y_{i+1} - y_i)^2 - (x - x_{i+1})^2 - (y - y_{i+1})^2}{2\sqrt{(x - x_i)^2 + (y - y_i)^2}\sqrt{(x_{i+1} - x_i)^2 + (y_{i+1} - y_i)^2}}\right)$$

$$\gamma_i = \arccos\left(\frac{(x_{i+1} - x_i)^2 + (y_{i+1} - y_1)^2 + (x - x_{i+1})^2 + (y - y_{i+1})^2 - (x - x_i)^2 - (y - y_i)^2}{2\sqrt{(x_{i+1} - x_i)^2 + (y_{i+1} - y_i)^2}\sqrt{(x - x_{i+1})^2 + (y - y_{i+1})^2}}\right)$$

Similarly, while calculating, for more complex shapes, such as Fig. 1e and f, it simply requires changing the superscript of the summation from 4 to 6, i.e., the number of sides of the polygon N. Compared to [12], the present paper aligns with its calculation when the field points are located inside the convex polygon, while for other shapes (concave polygons and self-intersecting polygons) or when the field points are located outside the charged plane, the calculations are very different. It is also worth noting that the triangular division of the polygon in [12] seems to be imperfect, and the number of triangles divided at different positions of the field point varies, making it impossible to obtain a specific analytical expression for the potential at any point in the plane. However, the method in this paper has a uniform division principle, the internal and external cases can be discussed simultaneously, and the results of the analytical expressions are generalized.

4 Spatial potential of a uniformly charged polygon

Let the triangle lie in the XOY plane, one vertex coincides with point O, one side lies on the $\boldsymbol{x}$ axis, and the length of the side opposite point O is $\boldsymbol{a}$. The included angles of triangles are recorded as α, β and γ in counterclockwise order. $\boldsymbol{X}$ is the intercept of the line where $\boldsymbol{a}$ is located on the $\boldsymbol{x}$ axis, and $\boldsymbol{H}$ is the height of the triangle perpendicular to the $\boldsymbol{a}$ side, as shown in Fig. 3.

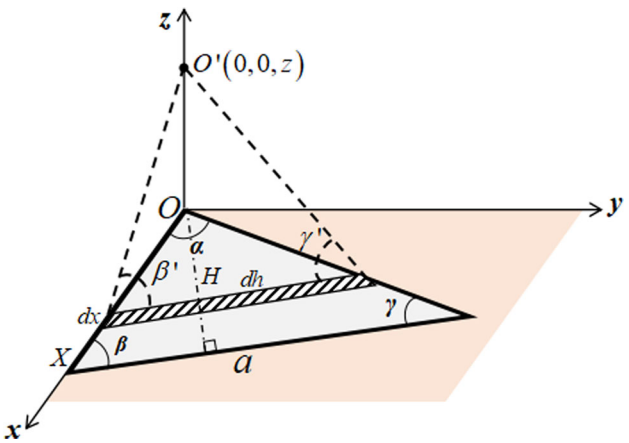

Fig. 3 Schematic diagram of triangle space located in XOY plane with vertices located at origin

Facing the difficulty that the selection of point charge microelements in Cartesian coordinate system involves elliptic integrals and it is impossible to solve the potential of an asymmetric triangle, the students, through in-depth thinking and extensive discussion, proposed to take a slender infinitesimal element parallel to the side a in the triangle. The potential of this micro-element (line density of charge $\lambda = \sigma dh = \sigma \sin\beta dx$) at the point $O'(0, 0, z)$ is [13]:

$$dV(0,0,z) = \frac{\lambda}{4\pi\varepsilon_0} \ln\left(\cot\left(\frac{\beta'}{2}\right)\cot\left(\frac{\gamma'}{2}\right)\right) \tag{6}$$

Here, respectively, β' and γ' are the two base angles of the triangle formed by the micro-element of this line and the point O'. This can be written specifically as:

$$\beta' = \arccos\frac{x cos\beta}{\sqrt{x^2+z^2}},\ \gamma' = \arccos\frac{x\sin\alpha/\sin\gamma - x\cos\beta}{\sqrt{x^2 - 2x^2\frac{\sin\alpha}{\sin\gamma}\cos\beta + x^2\frac{\sin^2\alpha}{\sin^2\gamma} + z^2}}$$

Thus, the potential on the perpendicular line $O'(0, 0, z)$ of the vertex of the uniformly charged triangle can be written as:

$$\begin{aligned} V(0,0,z) &= \frac{\sigma}{4\pi\varepsilon_0}\int_0^H \frac{dh}{4\pi\varepsilon_0}\ln\left(\cot\left(\frac{\beta'}{2}\right)\cot\left(\frac{\gamma'}{2}\right)\right) \\ &= \frac{\sigma}{4\pi\varepsilon_0}\left\{\begin{array}{l} H\ln(\sqrt{H^2\csc^2\beta + z^2} + H\cot\beta) \\ +H\ln(\sqrt{H^2\csc^2\gamma + z^2} + H\cot\gamma) \\ +2|z|\left[\arctan\left(\tan\left(\frac{\beta}{2}\right)\tan\left(\frac{1}{2}\arctan\left(\frac{H}{|z|\sin\beta}\right) - \frac{\pi}{4}\right)\right) + \frac{\beta}{2}\right] \\ +2|z|\left[\arctan\left(\tan\left(\frac{\gamma}{2}\right)\tan\left(\frac{1}{2}\arctan\left(\frac{H}{|z|\sin\gamma}\right) - \frac{\pi}{4}\right)\right) + \frac{\gamma}{2}\right] \\ -H\ln(H^2+z^2) - 2z\arctan\left(\frac{H}{z}\right)\end{array}\right\} \end{aligned} \tag{7}$$

The derivation of Eq. (7) is provided in Appendix B. Using Eq. (1) (7) for the potential at the same field point for the triangle of the literature [9], the numerical results obtained are in perfect agreement with [7] and the direct integration results [14]. Also considering that the method used in this paper is valid for arbitrary polygons and any field point, the results for triangles obviously lack sufficient representativeness, so the choice is still made to study them in terms of arbitrary quadrilaterals. Similarly, for an arbitrary uniformly charged quadrilateral $\boldsymbol{A_1A_2A_3A_4}$ in the XOY plane (Fig. 1a–d), it can be equivalent to the potentials on the perpendicular lines at the vertices of four triangles, so its potential at any point (x, y, z) in space can be analytically expressed as:

$$V(x,y,z) = \frac{\sigma}{4\pi\varepsilon_0}\sum_{i=1}^{4}\left\{\begin{array}{l} \delta_i\left\{H_i\ln(\sqrt{H_i^2\csc^2\beta_i + z^2} + H_i\cot\beta_i)\right. \\ +H_i\ln(\sqrt{H_i^2\csc^2\gamma_i + z^2} + H_i\cot\gamma_i) \\ +2|z|\left[\arctan\left(\tan\left(\frac{\beta_i}{2}\right)\tan\left(\frac{1}{2}\arctan\left(\frac{H_i}{|z|\sin\beta_i}\right) - \frac{\pi}{4}\right)\right) + \frac{\beta_i}{2}\right] \\ +2|z|\left[\arctan\left(\tan\left(\frac{\gamma_i}{2}\right)\tan\left(\frac{1}{2}\arctan\left(\frac{H_i}{|z|\sin\gamma_i}\right) - \frac{\pi}{4}\right)\right) + \frac{\gamma_i}{2}\right] \\ \left. -H_i\ln(H_i^2+z^2) - 2z\arctan\left(\frac{H_i}{z}\right)\right\}\end{array}\right\} \tag{8}$$

Since the point $(x, y, 0)$ is the projection of the point (x, y, z) in the XOY plane, the coefficients of Eq. (8) and Eq. (5) are then identical, and it is easy to verify that Eq. (8) degenerates to Eq. (5) when $z \to 0$.

It can be seen that the number of triangle combinations and divisions using the external division method are unique and are applicable to uniformly charged planes with arbitrary unsmooth edges, giving a clear advantage in the range of use. Whereas if the polygon is divided internally into a number of triangles, like [7], although there is no need to additionally fill in the blanks, there are various combinations of triangle divisions regarding concave polygons for which the calculus cannot be standardized, and for more complex shapes (e.g., stars) the conventional internal division approach will probably fail. Then from a methodological point of view, Kim et al.[7] use the barycentric coordinate system to create a linear representation of the coordinates of any point on the polygon plane and its vertex coordinates through a complex matrix. Although some sophisticated mathematical skills may be used to obtain its analytic results, the increase in the number of edges makes the transformation matrix extremely complex and no longer tractable, and basically can only rely on the results of some special cases to be added up. However, the mathematical treatment of Eq. (7) in the ordinary coordinate system is not difficult for students of electrical and electronic engineering due to the selection of appropriate microelements.

5 Applications

(1) In order to better understand and observe the physical meaning implied by Eq. (2), shapes containing homogeneous features are generally chosen as objects of study. Among them, regular polygon and circle are the most special cases of the polygon, which are characterized by high symmetry and are often used as classic teaching cases of electric potential and electric field. And based on the characteristics of the regular polygon, where the center and vertex define the threshold of physical quantities associated with them, the potential at any point in the plane lies between the potential at its center and the potential at its edges. As an application of the above discussion on the potentials of uniformly charged N-sides, the analytical solutions of the potentials of the centers and vertices of the regular N-sides can be obtained.

For a regular N-sided polygon, the relationship between the side length a and the radius R of the circumscribed circle is:

$$a = 2R\sin(\pi/N) \tag{9}$$

For the center, $\alpha = 2\pi/N$, $\beta = \gamma = (1/2\text{–}1/N)\pi$, $\delta_i = 1$. From Eq. (5), the potential of the center of the uniformly charged regular$N$-side polygon can be obtained as follows:

$$V_{NC} = \frac{N\sigma R\cos(\pi/N)}{2\pi\varepsilon_0}\ln\left(\sec\left(\frac{\pi}{N}\right)+\tan\left(\frac{\pi}{N}\right)\right) \tag{10}$$

For the vertex, $\alpha = \pi/N$, $\beta_k = (N\text{-}k\text{-}1)\pi/N$, $\gamma_k = k\pi/N$, $\delta_k = 1$, Similarly, from Eq. (5), the potential of the vertex of uniformly charged regular N-side polygon can be written as:

$$V_{NP} = \frac{\sigma R}{2\pi\varepsilon_0}\left[\sum_{k=1}^{N-2}\sin\left(\frac{k\pi}{N}\right)\sin\left(\frac{(k+1)\pi}{N}\right)\ln\left(\frac{\tan\left(\frac{(k+1)\pi}{2N}\right)}{\tan\left(\frac{k\pi}{2N}\right)}\right)\right] \tag{11}$$

The analytical solutions of the potentials of the centers and vertices of some uniformly charged regular N-side polygons are listed in Table 1 [4–8]. It can be seen that with the increase of N, the potential values increase and finally converge to the one of the circle ($N = \infty$).

Equations (10) and (11) summarize the potential solutions of the regular polygon and the circle into a unified expression, and the exact solution of the potential of the circular disk at any point can be obtained by means of the regular polygon convergence without the help of elliptic integrals. And it is verified numerically that Eq. (8) achieves good convergence accuracy when the number of sides is not too large. It is also observed that the difference between the central and edge potential potentials of the polygon changes accordingly with N when R is certain, with the difference reaching a maximum for $N = 5$, implying that the internal electric field of a charged plane with this shape is relatively the most complex.

(2) Specific images such as electric field lines and equipotential lines can make students better understand the concept of electric field and the relationship between field sources [15, 16]. Using Eqs. (5) and (8), the plane potential and space potential of the uniformly charged polygon can be calculated, and the potential distribution of the uniformly charged polygon can be visually expressed by depicting the intensity diagram of the potential and equipotential diagram [17]. Here, a concave quadrilateral **A** (Fig. 1c or d) and a self-intersecting quadrilateral **B** (Fig. 1e or f) are used as examples, where the coordinates of the vertices of **A** are $\boldsymbol{A_1}$ (0,0), $\boldsymbol{A_2}$ (0.5,0.5), $\boldsymbol{A_3}$ (1,0), $\boldsymbol{A_4}$ (0.5,1), and the coordinates of the vertices of **B** are $\boldsymbol{A_1}$ (0,0), $\boldsymbol{A_2}$ (1,0), $\boldsymbol{A_3}$ (0.5,0.5), $\boldsymbol{A_4}$ (1,1), $\boldsymbol{A_5}$ (0,1), $\boldsymbol{A_6 = A_3}$.

According to the intensity diagram of the potential and equipotential line in Fig. 3, it can be found that the relatively higher potential will be concentrated in the charged plane, and it will have the same characteristics for asymmetric triangles [18]. The shape of some equipotential lines (e.g., the red curve) is consistent with the real shape of the charged plane, but the vertices of the polygon do not necessarily lie on the same equipotential line. The maximum value (absolute value) of the potential is not always located at a particular point such as the geometric center of the graph, e.g., graph **B** contains two maximum points.

In fact, the shape of the equipotential lines in graph **B** is more specific, it can be seen that there is a critical potential $V_C = 1.76$ (at this time, the two equipotential lines approach infinitely at points (0.5, 0.5, 0)), which makes the equipotential lines corresponding to the same potential change from one to two. When $V < V_C$, it corresponds to the outer equipotential line of the critical equipotential line (red curve), and gradually expands outward with the equipotential line, and becomes a gourd-shaped closed curve with convex at both ends and concave in the middle. When $V > V_C$, there exist two equipotential lines, which correspond to the same potential. In general, the critical potential occurs possible for charged polygon with complex geometry.

Comparison of Figs. 4 and 5, it can be seen that as the vertical distance z of the field point from the plane becomes farther, the change amount of potential in the x or y direction decreases, so the contrast of the intensity diagram of potential also decreases. At the same time, the bending degree of the equipotential line at $z = 0.1$ is much weaker than that at $z = 0$, and the curves at $z = 0.1$ tend to be smooth. For example, the shape of the equipotential line (red curve) corresponding to the relatively high potential in Figs. 4a and 5a has changed from a heart shape to a triangle, which is far from the true shape of the charged plane.

If the potential of discrete charged planes with the same charge surface density is further calculated using Eq. (8), it can be found that the equipotential line still reflects the charge distribution characteristics of the charged body. In particular, when uniformly

Table 1 Analytical solutions of the potentials of centers and vertices of regular N-side polygons (using reduced potential $\tilde{V} = 4\pi\varepsilon_0 V/\sigma R$)

N	$\tilde{V}$	
	$\tilde{V}_C$	$\tilde{V}_P$
3	$3\ln\left(2+\sqrt{3}\right)$ (≈ 3.951)	$\frac{3}{2}\ln 3$ (≈ 1.648)
4	$4\sqrt{2}\ln\left(\sqrt{2}+1\right)$ (≈ 4.986)	$2\sqrt{2}\ln\left(\sqrt{2}+1\right)$ (≈ 2.493)
5	$\frac{5\left(\sqrt{5}+1\right)}{2}\ln\left(\frac{4+\sqrt{10-2\sqrt{5}}}{\sqrt{5}+1}\right)$ (≈ 5.455)	$\frac{\sqrt{5}}{2}\ln 5+\frac{5+\sqrt{5}}{4}\ln\left(\frac{3+\sqrt{5}}{5-\sqrt{5}}\right)$ (≈ 2.955)
6	$3\sqrt{3}\ln 3$ (≈ 5.709)	$\sqrt{3}\ln\left(3+2\sqrt{3}\right)$ (≈ 3.232)
8	$8\sqrt{2+\sqrt{2}}\ln\left(\sqrt{4-2\sqrt{2}}+\sqrt{2}-1\right)$ (≈ 5.960)	$\sqrt{4-2\sqrt{2}}\ln\left(\sqrt{4-2\sqrt{2}}+1\right)$ $+\sqrt{4+2\sqrt{2}}\ln\left(\frac{2-\sqrt{2-\sqrt{2}}}{\sqrt{2-\sqrt{2}}}\right)$ $+\sqrt{2+\sqrt{2}}\ln\left(\frac{2+\sqrt{2-\sqrt{2}}}{2-\sqrt{2-\sqrt{2}}}\right)$ (≈ 3.534)
12	$6\left(\sqrt{2}+\sqrt{6}\right)\ln\left(\sqrt{6}-\sqrt{2}+2-\sqrt{3}\right)$ (≈ 6.140)	$\sqrt{2}\ln\left(2\sqrt{3}+1-\sqrt{6}\right)+\sqrt{6}\ln\left(\frac{3+\sqrt{6}}{3}\right)$ $+\frac{\sqrt{6}-\sqrt{2}}{2}\ln\left(1-\sqrt{2}+\sqrt{6}\right)$ $+\frac{\sqrt{6}+3\sqrt{2}}{2}\ln\left(3\sqrt{2}-\sqrt{6}-2\sqrt{3}+3\right)$ (≈ 3.772)
Circular	2π	4

charged planes with different shapes are placed in stacks, the equipotential surface qualitatively reflects the shape of a three-dimensional uniformly charged body by observing how similar the equipotential lines corresponding to the same potential are to the shape of the cross section.

6 Teaching assessment

The purpose of teaching reform is to improve teaching. To test the results of this teaching in small group peer learning, it is necessary to get feedback from the students after class [19, 20]. By understanding what confuses students and how they embrace the new teaching methods, it propels the teaching to move forward. By applying the small group teaching of college physics at the University of Electronic Science and Technology of China, a total of 30 students in this class were asked to independently respond to 10 questions set out in a post-class feedback form (Table 2), ranging from personal knowledge base to pedagogical relevance. A scale of 1–5 was used as a rubric, representing 'strongly disagree,' 'disagree,' 'neither agree nor disagree (neutral),' 'agree ,' and 'strongly agree,' with a mean score closer to 5 meaning that students agree more with this and vice versa. Questions 1–3 were designed to collect the students' level of understanding and mastery of their past knowledge, to provide suggestions for better reinforcement and targeted teaching improvement based on the knowledge the students had before this lesson, and also the reason for choosing this integration method for solving the potential in this paper. Questions 4–7 are a comparison with other methods, the specific views of the students on this topic of research, to obtain how students accept the solution of the spatial potential in this paper, and the significance of the research in this paper. Questions 8–10 are from a larger educational and pedagogical perspective, to measure the unique advantages of Peer Learning over traditional teaching and learning, illustrating the need for continuous innovation in teaching methods.

It is shown in Table 2 that although students have some calculus skills and are aware of the unique advantages of the superposition theorem in solving complex charged bodies, they are often limited in a global integral (i.e., a form of internal integration) by the influence of the potential integral form when they encounter complex problems. At the same time, the choice of microelement is

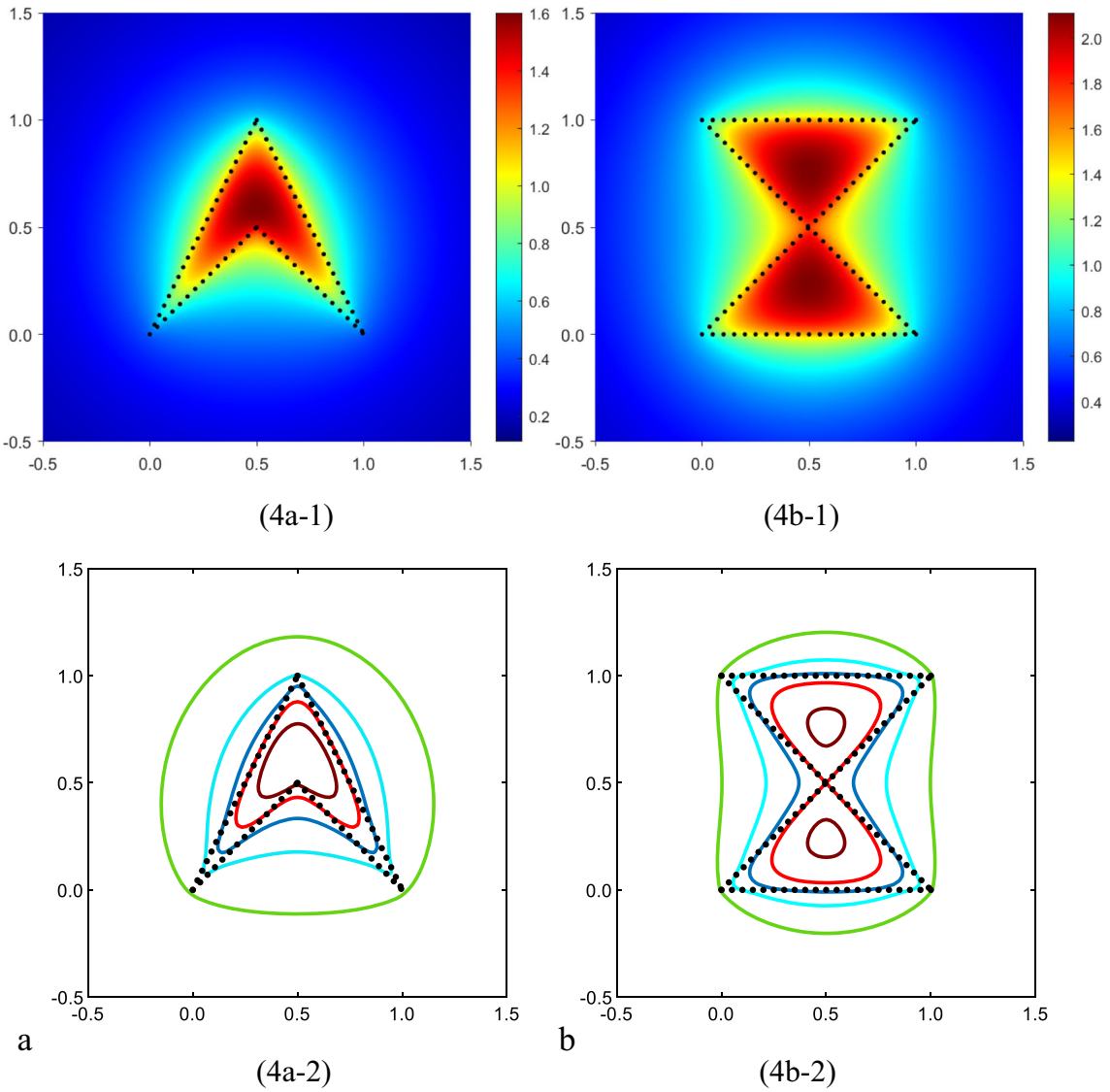

Fig. 4 Intensity diagrams and equipotential lines of uniformly charged concave quadrilateral (**a**) and self-intersecting quadrilateral (**b**) when $z = 0$. Different color curves represent potential values from inside to outside as follows: (4a-2) 1.20, 1.00, 0.80, 0.60, 0.40. (4b-2) 2.06, 1.76, 1.46, 1.16, 0.86. The horizontal and vertical axes represent coordinates x and y, respectively (the same as later). The dotted line indicates the shape of the original quadrilateral

extremely dependent on the shape of the object, and thus the lack of a more general one that is applicable to any shape has led to unsatisfactory results. Students can only analyze and discuss highly symmetric shapes. What's more, as most of the students found the analytical expressions to be more physically meaningful than the numerical results, they seemed to be more likely to observe some of the details embedded in the analytical results, and were more willing to accept uniform and relatively simple results for the expressions, which firmly established the importance of this paper on the methodological innovation in the solution of the space potential with Eq. (8). Furthermore, to decompose a complex structure into a finite number of solvable elementary units, like a black box, it is necessary to avoid the unmeasurable interior and consider only a limited amount of boundary point information. This not only teaches students to learn to split and integrate when encountering physical problems, but also provides a good solution for studying complex connected graphs. And finally, by combining the theoretical results with computer simulation by means of analytical expressions, the potential distribution characteristics of arbitrary graphs can be obtained conveniently and intuitively, which further confirms the high dependence relationship between field sources.

In terms of the final teaching effect, the peer learning method of choosing a small group of students from different majors who are all interested in physics and electrical engineering is a typical kind of mutual supportive learning, which has very many advantages. Although the topic is more challenging than the textbook, the advantage is that during the group discussion, the students are able to pool their ideas and bring out their own strengths, and the methods used are basically suggested by the students. Thus, a solution that is best understood and accepted by the general public can be obtained and the students can have a deeper understanding of

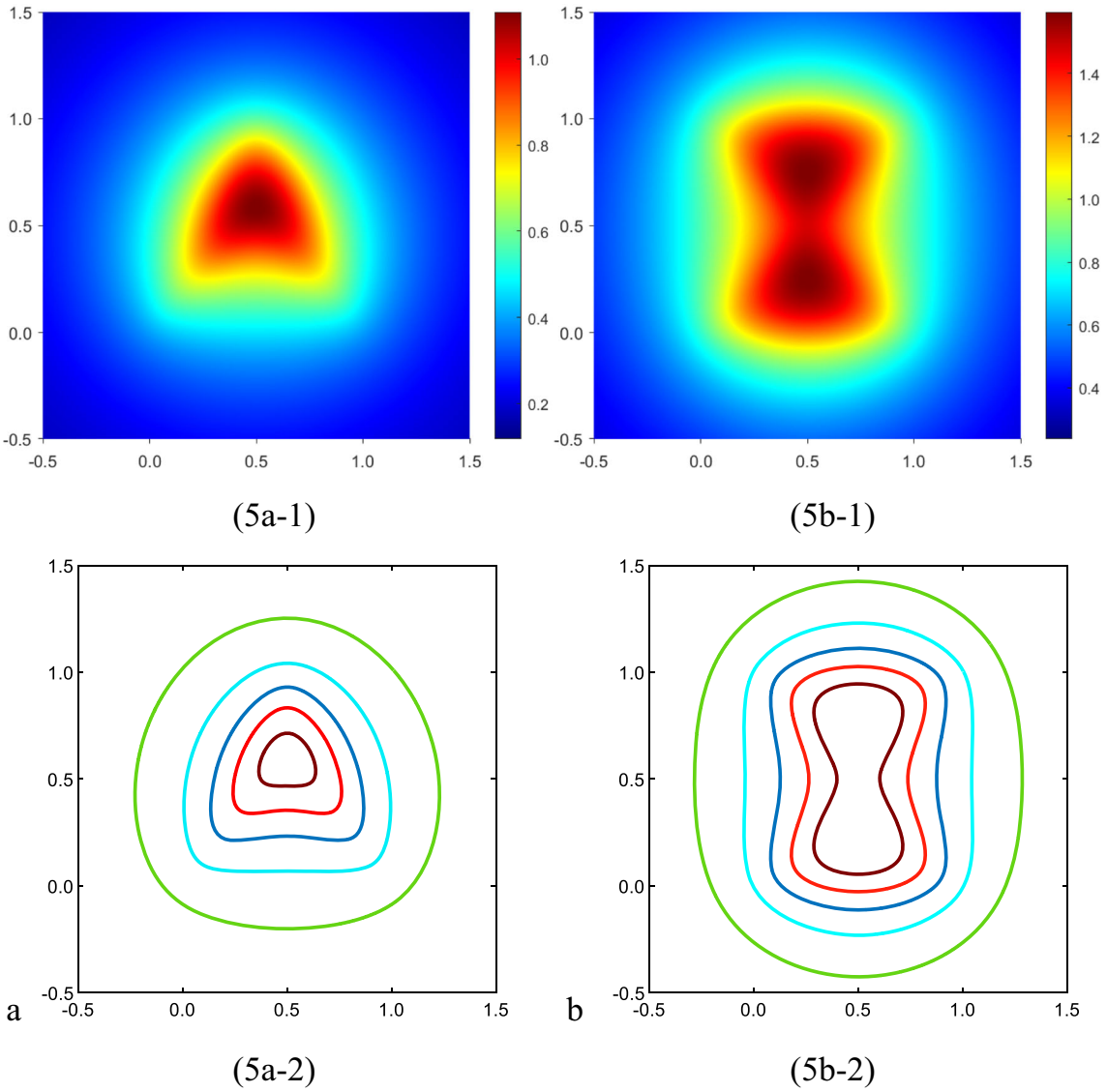

Fig. 5 Intensity diagrams and equipotential lines of uniformly charged concave-convex quadrilateral (**a**) and self-intersecting quadrilateral (**b**) when $z = 0.1$. Different color curves represent potential values from inside to outside as follows: (5a-2) 1.03,0.86,0.69,0.52,0.35; (5b-2) 1.40,1.20,1.00,0.80, 0.60

the knowledge. At the same time, the collaborative group approach allows students to be more proactive than traditional teaching methods, and multidisciplinary learning fosters teamwork [21]. The hands-on approach also gives students a clearer purpose for their learning, and to some extent lays the foundation for future scientific research.

7 Summary

According to the potential superposition theorem, an external division mode is determined to divide an arbitrary N-sided polygon into N triangles in this article. Thus, the plane potential of uniformly charged N-sided polygon is equivalent to the electric potentials at the vertices of N uniformly charged triangles, and further the space potential of uniformly charged N-sided polygon is equivalent to the potential on the perpendicular lines at the vertices of N triangles. Therefore, the analytical expression of the space potential of any uniformly charged polygon is obtained. As applications, the potential of the center and vertex of a uniformly charged regular N-sided polygon is calculated, and the equipotential lines of plane potential and space potential of the N-sided polygon are drawn at the same time.

Compared with the barycentric coordinate system, the analytical expressions of plane and space potential in this paper are more convenient, and the derivation process of all equations in this paper is rather easier, only involving elementary functions, which can be well understood and accepted by most undergraduates. In this paper, the calculation of the spatial potential integral for an

Table 2 Students' feedback on this lesson

Number	Question	Score	1	2	3	4	5	Average
1.	Before this course, I can make reasonable use of the principle of superposition to solve for the potential of charged bodies		4	6	9	9	2	2.97
2.	Before this course, I can choose a reasonable number of microelements and coordinate systems to simplify integration and avoid singularities		4	12	8	5	1	2.57
3.	Before this course, I had only solved the potential distribution of highly symmetrical shapes, such as rectangles and disks		0	3	6	8	13	4.03
4.	I prefer complete and uniform expression results to categorical discussion cases		1	3	3	13	10	3.93
5.	I prefer the method proposed in this paper to numerical integration and other methods		2	6	8	11	3	3.23
6.	The solution ideas in this paper have inspired me to solve other complex problems to some extent		0	7	9	12	2	3.30
7.	The combination of simulation and calculation has given me a deeper understanding of electrostatic fields than traditional teaching		4	5	5	11	5	3.27
8.	I believe that peer learning is a more effective way of obtaining relatively simple and popular methods and results		0	4	3	15	8	3.90
9.	Peer learning has made me more active in scientific research		0	8	6	14	2	3.33
10.	The active learning process, based on the material and practice, can promote my interest in scientific research compared to traditional teaching		2	3	10	11	4	3.40

N-sided shape is reduced to the summation of N expressions, using only the boundary point information without considering the internal integration region, which greatly simplifies the computational workload and avoids the creation of singularities, especially for irregular shapes, an advantage that is extremely obvious. In addition, all parameters in the expressions are easily accessible and have high circular symmetry, and all the numerical calculations are very convenient with the aid of a computer. At the same time, the equipotential lines of complex polygons drawn in this paper can qualitatively reflect the actual shape and charging characteristics of charged bodies to a certain extent, which ensures students a more intuitive understanding of the field-source relationship of charged bodies. As one of the important components in electronic engineering, capacitors have uniformly charged pole plates, so, the results of this paper can also provide a valuable reference for the electronics manufacturing field, and understanding the electric field distribution laws is beneficial for targeting improvements in the performance.

Finally, the above case study is the result of an independent extension research achieved by carrying out the cooperative learning model of student groups based on the content of the university physics course in the freshmen and the sophomores of the University of Electronic Science and Technology. Compared with traditional teaching, it adds numerous aspects such as students' independent choice of topics, extensive discussions, literature review, practical application of mathematical and scientific knowledge, simulations, teacher-student interaction and so on. This peer learning approach not only increases students' interest in learning physics and improves the efficiency of problem solving, but the analysis process and results are often more profound and easily accepted by the students. The organic integration of theory, simulation and practice in the classroom allow students to consolidate their scientific knowledge and at the same time develop their scientific skills in all aspects, laying good foundations for future scientific research.

Acknowledgements The authors would like to express their gratitude to Professor Qingsheng Zhu and Professor Minghe Wu from the School of Physics at the University of Electronic Science and Technology of China for their valuable insights and discussions on this article. Additionally, the authors extend their appreciation to all the students of the 2020 Yingcai Class who participated in the teaching evaluation.

Author's contribution CS: Conceptualization, Methodology, Writing-Qriginal Draft. LJ: Writing-Qriginal Draft. CX: Software, Data Curation. WY: Investigation. TB: Writing-Review&Editing.

Data Availability Statement This manuscript has associated data in a data repository. [Authors' comment: The authors declare that the data supporting the findings of this study are available within the paper.]

Appendix A

As shown in Fig. 6, let us assume that the triangle lies in the XOY plane. One of the vertices coincides with the origin O, and one of the sides lies on the x-axis. The length of the side opposite origin O is $\boldsymbol{a}$, and the angles within the triangle are denoted as α, β, and γ in counterclockwise order.

The $\boldsymbol{X}$ represents the intercept of the line with a length of a on the x-axis, and $\boldsymbol{H}$ is the height of the triangle perpendicular to the side $\boldsymbol{a}$. We take an infinitesimal strip element on this triangle in the direction parallel to the side $\boldsymbol{a}$, with a width of dh. This element can be considered as a uniformly charged finite line segment with a charge linear density of $\lambda = \sigma dh$.

First, we take a differential segment of the line element with a length da on this line element. Then, based on the point element obtained here, we calculate the electric potential produced by the infinitesimal line segment element at the origin O.

$$dVL(0,\,0) = \lambda da/4\pi\varepsilon_0 r$$

where r is the distance from the differential element to the origin O. Based on the geometric relationships: $r = h\csc\theta$, $a = h\cot\theta$, thus, the electric potential at the origin by the infinitesimal line element with uniform charge distribution is:

$$VL(0,\,0) = \int_{\pi-\gamma}^{\beta} \frac{\lambda d(h\cot\theta)}{4\pi\varepsilon_0 h\csc\theta} = \frac{\lambda}{4\pi\varepsilon_0}\int_{\beta}^{\pi-\gamma} \csc\theta d\theta = \frac{\lambda}{4\pi\varepsilon_0}\ln\left(\cot\left(\frac{\beta}{2}\right)\cot\left(\frac{\gamma}{2}\right)\right)$$

The above equation employs the integral formula $\int \csc\theta d\theta = \ln|\tan(x/2)| + const$, thereby, the electric potential at the vertex of the uniformly charged triangle is:

$$V(0,\,0) = \frac{\sigma}{4\pi\varepsilon_0}\ln\left(\cot\left(\frac{\beta}{2}\right)\cot\left(\frac{\gamma}{2}\right)\right)\int_0^H dh = \frac{\sigma a\sin\beta\sin\gamma}{4\pi\varepsilon_0\sin\alpha}\ln\left(\cot\left(\frac{\beta}{2}\right)\cot\left(\frac{\gamma}{2}\right)\right)$$

where $X = a\sin\gamma/\sin\alpha$, $H = X\sin\beta = a\sin\beta\sin\gamma/\sin\alpha$.

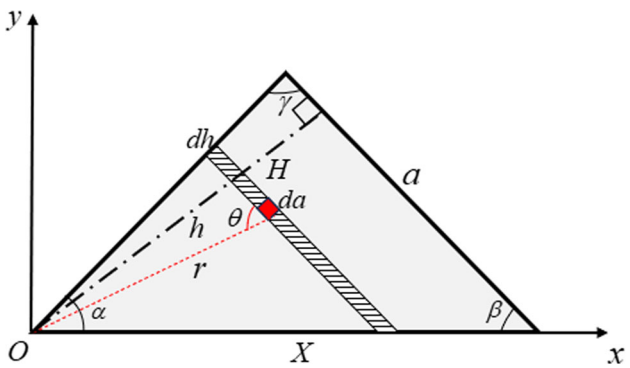

Fig. 6 Triangle in the XOY Plane with the Vertex at the Origin

Appendix B

Applying an identity transformation to Eq. (6):
$\cot(\theta/2) = (1+\cos\theta)/\sin\theta$, $\cos(\arccos(u)) = u$, $\sin(\arccos(u)) = \sqrt{1-u^2}$,
Hence, the integral expression for electric potential can be written as:

$$\begin{aligned} V(0,\,0,\,z) &= \frac{\sigma}{4\pi\varepsilon_0}\int_0^X \ln\left(\cot\left(\frac{\beta'}{2}\right)\cot\left(\frac{\gamma'}{2}\right)\right)dx\sin\beta \\ &= \frac{\sigma\sin\beta}{4\pi\varepsilon_0}\int_0^X \ln\left(\frac{1+\cos\beta'}{\sin\beta'}\right)dx + \frac{\sigma\sin\beta}{4\pi\varepsilon_0}\int_0^X \ln\left(\frac{1+\cos\gamma'}{\sin\gamma'}\right)dx \\ &= I(\alpha,\,\beta,\,\gamma) + I(\alpha,\,\gamma,\,\beta) \end{aligned}$$

The calculations can be simplified using the symmetry of β and γ.

$$\begin{aligned} I(\alpha,\,\beta,\,\gamma) &= \frac{\sigma\sin\beta}{4\pi\varepsilon_0}\int_0^X \ln\left(\frac{\sqrt{x^2+z^2}+x\cos\beta}{\sqrt{x^2\sin^2\beta+z^2}}\right)dx \\ &= \frac{\sigma\sin\beta}{4\pi\varepsilon_0}\left\{\int_0^X \ln\left(\sqrt{x^2+z^2}+x\cos\beta\right)dx - \frac{1}{2}\int_0^X \ln\left(x^2\sin^2\beta+z^2\right)dx\right\} \\ &= \frac{\sigma\sin\beta}{4\pi\varepsilon_0}\left\{\begin{array}{l} X\ln\left(\sqrt{X^2+z^2}+X\cos\beta\right) - \displaystyle\int_0^X \frac{x^2+x\cos\beta\sqrt{x^2+z^2}}{x^2+z^2+x\cos\beta\sqrt{x^2+z^2}}dx \\ -\dfrac{1}{2}X\ln\left(X^2\sin^2\beta+z^2\right) + \displaystyle\int_0^X \frac{x^2\sin^2\beta}{x^2\sin^2\beta+z^2}dx \end{array}\right\} \end{aligned}$$

The equation above utilizes integration by parts: $\int udv = uv - \int vdu$. Next, we calculate the two definite integrals inside the right parenthesis.

$$\begin{aligned} &\int_0^X \frac{z^2}{x^2+z^2+x\cos\beta\sqrt{x^2+z^2}}dx \;\underline{\underline{x = z\tan u}}\; \int_0^{\arctan(X/z)} \frac{z}{1+\cos\beta\sin u}du \\ &= \frac{2z}{\sin\beta}\left\{\arctan\left(\tan\left(\frac{\beta}{2}\right)\tan\left(\frac{1}{2}\arctan\left(\frac{X}{z}\right)-\frac{\pi}{4}\right)\right)+\frac{\beta}{2}\right\} \\ &\int_0^X \frac{z^2}{x^2\sin^2\beta+z^2}dx = \frac{z}{\sin\beta}\arctan\left(\frac{\sin\beta}{z}X\right) \end{aligned}$$

The equation above is further simplified using the half-angle formula,
$\tan(\theta/2) = \sqrt{(1-\cos\theta)/(1+\cos\theta)}$,
and referring to the integral table, we have:

$$\begin{aligned} &(\,c > d,\ \int \frac{1}{c+d\sin t}dt = \frac{2}{\sqrt{c^2-d^2}}\arctan\left(\frac{c\tan(t/2)+d}{\sqrt{c^2-d^2}}\right)+const \\ &\text{or } \int \frac{1}{c+d\sin t}dt = \frac{2}{\sqrt{c^2-d^2}}\arctan\left(\sqrt{\frac{c-d}{c+d}}\tan\left(\frac{t}{2}-\frac{\pi}{4}\right)\right)+const, \\ &\text{and } \int \frac{1}{t^2+c^2}dt = \frac{t}{c}\arctan\left(\frac{t}{c}\right)+const\,) \end{aligned}$$

Organizing all the components and simplifying, we obtain Eq. (7).

References

1. W.A. Anderson, U. Banerjee, C.L. Drennan et al., Changing the culture of science education at research universities. Science **331**(6014), 152–153 (2011)
2. S. Myllymaki, Cooperative learning in lectures of an advanced electrical engineering course. Int. J. Electr. Eng. Educ. **49**(2), 146–156 (2012)
3. R.P. Feynman, R.B. Leighton and M.L. Sands, *The Feynman Lectures on Physics vol 2* (Reading, MA: Addison-Wesley) (1965)
4. E.M. Purcell, *Electricity and Magnetism: Berkeley Physics Course vol 2 2nd ed* (*In SI units*)(Singapore: McGraw-Hill) (2014)
5. O. Ciftja, B. Ciftja, Results for the electrostatic potential of a uniformly charged square plate. Res. Phys. **19**, 103671 (2020)
6. O. Ciftja, Electrostatic potential of a uniformly charged square plate at an arbitrary point in space. Phys. Scr. **95**, 095802 (2020)
7. U.R. Kim, W. Han, D.W. Jung, J. Lee, C. Yu, Electrostatic potential of a uniformly charged triangle in barycentric coordinates. Eur. J. Phys. **42**, 045205 (2021)
8. V. Bochko, Z.K. Silagadze, On the electrostatic potential and electric field of a uniformly charged disk. Eur. J. Phys. **41**, 045201 (2020)

9. E.E. Okon, R.F. Harrington, The potential due to a uniform source distribution over a triangular domain. Int. J. Numer. Meth. Eng. **18**(9), 1401–1411 (1982)
10. P.J. Davis, P. Rabinowitz, *Methods of Numerical Integration*, 2nd edn. (Academic Press, New York, 1975)
11. R.J. Duffin, J.H. McWhirter, A formula for the potential of a polygon with varying charge density. J. Franklin Inst. **316**(6), 451–466 (1983)
12. A. Aghamohammadi, Dimensional analysis and electric potential due to a uniformly charged sheet. Eur. J. Phys. **32**, 633 (2011)
13. R.J. Rowley, Finite line of charge. Am. J. Phys. **74**(12), 1120–1125 (2006)
14. D.R. Ferreira, A brief comment on the numerical results in 'Electrostatic potential of a uniformly charged triangle in barycentric coordinates.' Eur. J. Phys. **42**(6), 068001 (2021)
15. E. Campos, G. Zavala, K. Zuza, J. Guisasola, Electric field lines: the implications of students' interpretation on their understanding of the concept of electric field and of the superposition principle. Am. J. Phys. **87**(8), 660–667 (2019)
16. E. Campos, G. Zavala, K. Zuza, J. Guisasola, Students' understanding of the concept of the electric field through conversions of multiple representations. Phys. Rev. Phys. Educ. Res. **16**(1), 010135 (2020)
17. H. Murata, M. Sakuraoka, Electrostatic potential on a laboratory measurement experiment. Am. J. Phys. **48**(9), 763–766 (1980)
18. U.R. Kim, W. Han, D.W. Jung, J. Lee, C. Yu, Reply to Comment on 'Electrostatic potential of a uniformly charged triangle in barycentric coordinates.' Eur. J. Phys. **42**(6), 068002 (2021)
19. R. Kang, Y. Lin, Y. Wang et al., A pedagogical case on active learning regarding to Kirchhoff's circuit laws. The Int. J. Electr. Eng. Educ. **56**(2), 179–190 (2019)
20. M. Ing, C. Victorino, Differences in classroom engagement of Asian American engineering students. J. Eng. Educ. **105**(3), 431–451 (2016)
21. M.C. Hersam, M. Luna, G. Light, Implementation of interdisciplinary group learning and peer assessment in a nanotechnology engineering course. J. Eng. Educ. **93**(1), 49–57 (2004)